Hyperspectral Image Projector for Advanced Sensor Characterization

S. W. Brown*, J. P. Rice, J. E. Neira, R. Bousquet, and B. C. Johnson
National Institute of Standards and Technology, Gaithersburg, MD, USA 20899

ABSTRACT

In this work, we describe radiometric platforms able to produce realistic spectral distributions and spatial scenes for the development of application-specific metrics to quantify the performance of sensors and systems. Using these platforms, sensor and system performance may be quantified in terms of the accuracy of measurements of standardized sets of complex source distributions. The same platforms can also serve as a basis for algorithm testing and instrument comparison. The platforms consist of spectrally tunable light sources (STS's) coupled with spatially programmable projection systems. The resultant hyperspectral image projectors (HIP) can generate complex spectral distributions with high spectral fidelity; that is, scenes with realistic spectral content. Using the same fundamental technology, platforms can be developed for the ultraviolet, visible, and infrared regions. These radiometric platforms will facilitate advanced sensor characterization testing, enabling a pre-flight validation of the pre-flight calibration.

Keywords: Calibration, hyperspectral, imaging, spectroscopy, radiometry

1. INTRODUCTION

Traditional calibration source standards such as lamp-illuminated integrating spheres are designed to be spatially uniform and have spectral properties that vary smoothly with wavelength. These are important characteristics leading to the consistent dissemination of standards with the lowest possible uncertainties. Remote sensing satellite sensors such as the Moderate Resolution Imaging Spectroradiometer (MODIS) and the Sea-viewing Wide Field-of-View Sensor (SeaWiFS) used lamp-illuminated integrating spheres to set the pre-launch gains of their reflected solar bands [1, 2]. Sensor calibration plans for future missions such as the National Polar-orbiting Operational Environmental Satellite System (NPOESS) Preparatory Project (NPP) and the NPOESS Visible Infrared Imaging Radiometer Suite (VIIRS) sensor also envision using a lamp-illuminated integrating sphere to establish the sensor channel gains in the solar reflective region [3].

Source characteristics such as spectral or spatial distribution, brightness, or temporal behavior all impact radiometric measurements. Ideally, remote sensing satellite sensors are characterized using a source with radiometric characteristics similar to those that will be seen on-orbit. This is due to the fact that many types of measurement bias exist in radiometry, and these effects are exacerbated when the calibration source and the target source differ in their fundamental influencing parameters. While the existing calibration sources are important for general applications and have served the remote sensing community well, they are markedly different from the scenes sensors view on-orbit. Those scenes are highly non-uniform and spectrally complex, with spectral distributions dissimilar to the spectral distributions of the calibration sources. In Fig. 1 we show the spectral distribution of a lamp-illuminated integrating sphere source (ISS) using quartz tungsten halogen (QTH) lamps operating at a color temperature of approximately 2856 K, a common operating point for QTH lamps. Also shown in the figure is the reflected solar radiation from the Earth for an albedo of 0.5 % and 80 %. Note the striking difference in the spectral distribution of the two sources. Lamp-illuminated integrating spheres have a uniform radiance distribution within the sphere exit port (typically uniform to within a few per cent). Fig. 2 shows the radiance distribution of a typical lamp-illuminated integrating sphere. In contrast, the Earth is a highly variable scene.

Radiometric uncertainty requirements in the reflected solar region for next generation satellite sensors involved in measurements of climate change, such as for data from sensors in the NPOESS program, are stringent. For example,

*Correspondence: swbrown@nist.gov

Earth Observing Systems XI, edited by James J. Butler, Jack Xiong,
Proc. of SPIE Vol. 6296, 629602, (2006) · 0277-786X/06/$15 · doi: 10.1117/12.682232

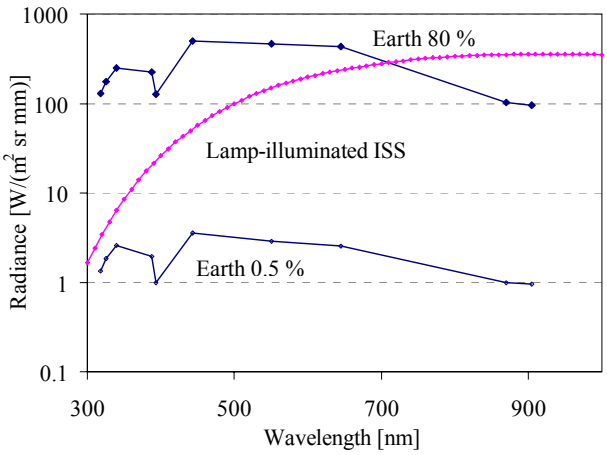

Fig. 1. Spectral distribution of a lamp-illuminated integrating sphere and the spectral distribution of reflected solar radiation for an Earth albedo of 0.5 % and 80 %, respectively. The data are plotted as points. The lines are a guide for the eye.

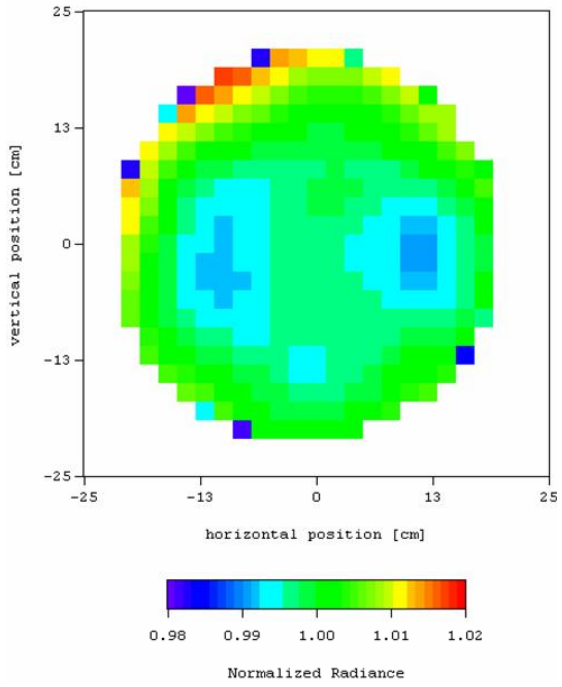

Fig. 2. Spatial uniformity of a 1-m diameter lamp-illuminated integrating sphere with a 50-cm diameter exit port.

satellite sensors must have the ability to measure atmospheric temperature trends as small as 0.1 ^{o}C/decade, ozone changes of 1 %/decade, and solar variability on the order of 0.1 %/decade [4]. For NPOESS, the operational paradigm is to rely on vendor supplied data products or environmental data records directly. Under these guidelines, the availability of relevant, application-specific, radiometric artifacts to evaluate and validate the performance of instruments in the laboratory prior to launch will be extremely valuable.

It is time-consuming, expensive, and often impractical to develop and maintain different sets of calibration artifacts for each type of calibration, or for each anticipated application of an instrument. This has motivated the concept of a unified, generalized radiometric calibration platform that can operate over a wide spectral range with at most modest changes to the basic structure. This platform will be used to generate a wide variety of different sets of standard calibration artifacts needed for advanced radiometric characterization and calibration of sensors. In addition to the reduction of uncertainties that arise from measurement bias, more efficient utilization of resources can be achieved by combining individual test, characterization, and calibration procedures that are required for a thorough understanding of a sensor's performance into procedures that utilize these advanced radiometric platforms.

In general, advanced calibration artifacts include spatially as well as spectrally complex distributions. Accordingly, there are two independent components to a full calibration platform capable of generating spatially and spectral complex scenes: a spectral component and a spatial component. Thus, a fully integrated radiometric characterization and calibration facility would have the capability of generating standardized sets of spatially complex scenes with high spectral fidelity [5].

In this work we combine the spectral and spatial elements in a Hyperspectral Image Projector (HIP). The HIP will be used to project standardized or user-definable scenes with high spectral fidelity. In Section 2, we describe the development of the first component of the HIP system, a Spectrally Tunable Source, capable of generating complex spectral distributions. In Section 3, we describe the concepts behind the development of the complete HIP system.

2. SPECTRALLY TUNABLE SOURCE (STS)

A variety of different approaches to the development of spectrally tunable sources have recently been described, including the use of spatial light modulators [5, 6] and light-emitting diodes (LEDs) [7]. In this work, we describe an STS based around a dispersing element and a spatial light modulator (SLM) [8]. STS's using a digital micro-mirror device (DMD) as the spatial light modulator have been developed for the visible [6, 8] and short-wave infrared spectral regions [5]. The foundation of the STS is shown in Fig. 3. The system is basically a spectrograph, with a spatial light modulator replacing the multi-element detector at the focal plane. In this case, the dispersed light falls on the SLM, creating a relationship between the spatial location on the SLM and the wavelength of the light. The spectral coverage is determined by the dispersing element and the size and placement of the SLM. The DMD's used in the STS have 1024 columns and 768 rows of 13.68 μm square aluminum coated elements, or pixels. By turning individual elements of the DMD comprising the SLM 'on', spectrally diverse distributions can be created. Broadband light is the incident light sent into the STS from a user-selected source. Narrowband light is light reflected from the DMD, collected, spatially homogenized, and coupled into a light guide. The silicon photodiode and Holmium Oxide wavelength reference standard filter, elements 11 and 12 in the figure, are for calibration of the spectral distribution and wavelength accuracy, respectively.

By turning individual columns or sets of columns on, one at a time, spectral distributions such as those shown in Fig. 4 are obtained. By turning a number of different columns on and measuring the wavelength of the collected radiation, a wavelength calibration can be obtained. The wavelength calibration, measured using a reference spectroradiometer, shown in Fig. 5, relates the column number on the DMD array to the peak wavelength of the reflected radiation. Use of this information, along with the intensity distribution within a column and from column-to column, illustrated in Fig. 6, allows algorithms to be developed to generate a spectral match to a given distribution. Varying the number of mirrors turned on from 0 to 768 in a particular column gives us a dynamic range of approximately 750 for each wavelength (assuming nearly uniform illumination of the DMD). High fidelity spectral matches to a specific target distribution can be readily achieved, with the resolution defined by the design and imaging properties of the spectrograph. The STS described in this work had a resolution of 10 nm.

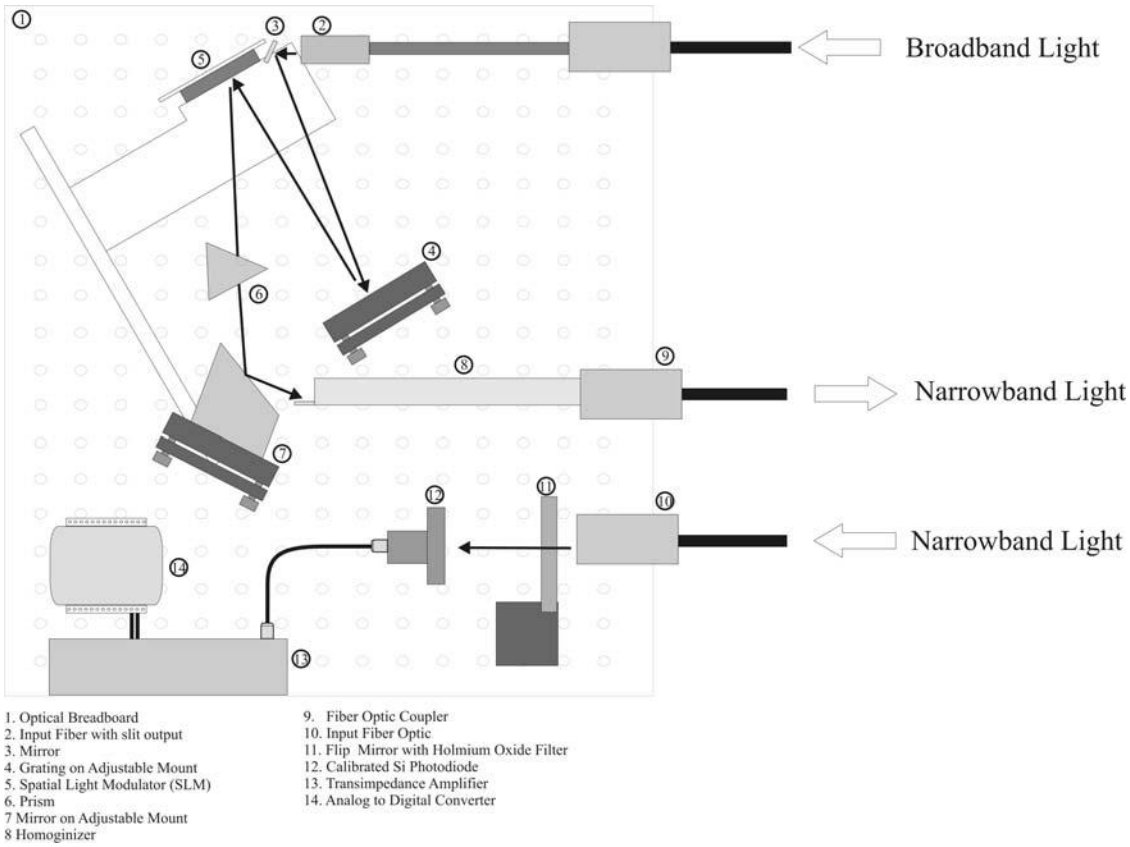

Fig. 3. Generalized conceptual schematic diagram of an STS. Broadband light is the incident light from a user-selected source. Narrowband light is light reflected from the DMD, collected, spatially homogenized, and coupled into a light guide. The silicon photodiode and wavelength standard reference are for calibration of the spectral distribution and wavelength accuracy, respectively.

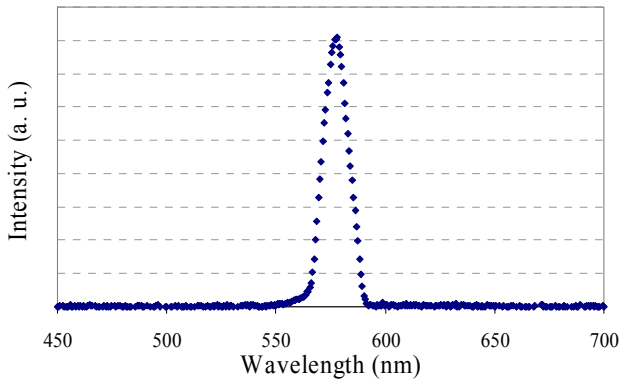

Fig. 4. Output of an STS with an individual set of 10 neighboring columns turned on.

The system in general is designed to have different source inputs. The input source can then be tailored to the intended application. Conventional quartz tungsten-halogen or Xe sources can be used, but newer sources such as LED-based sources or supercontinuum sources [9] can also be easily incorporated into the system.

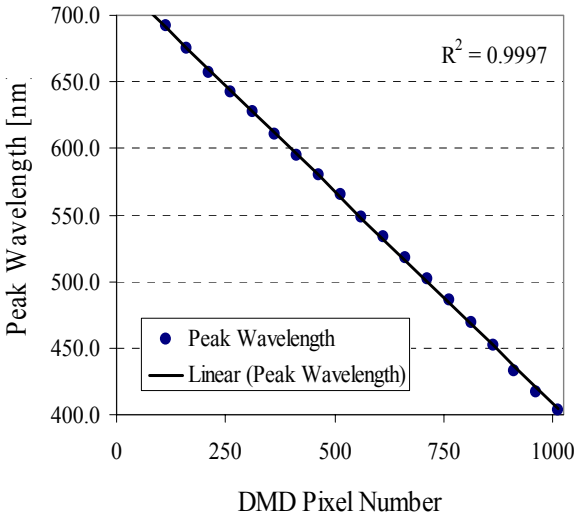

Fig. 5. Wavelength calibration of a visible STS.

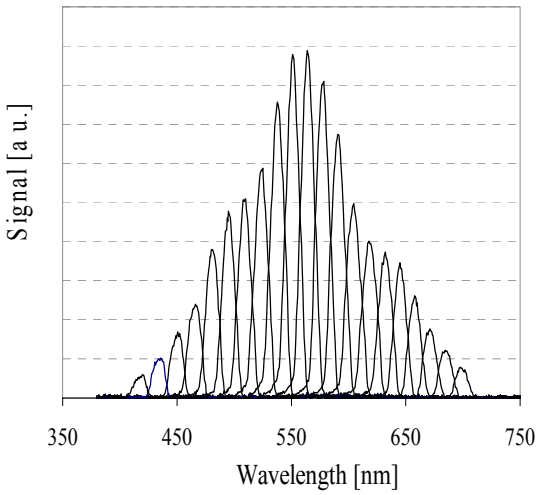

Fig. 6. Column-to-column intensity calibration of a visible STS.

Fig. 7 shows matches of the STS output to a Gaussian target spectral distribution and an ocean color spectral distribution using a quartz tungsten halogen lamp as the input source. This particular STS had a resolution of approximately 10 nm. Note that no iterative feedback was enabled for these spectral matches, and the DMD was assumed to be uniformly illuminated by the source. Even with these limiting assumptions, good spectral matches were obtained for these two very different target spectral distributions.

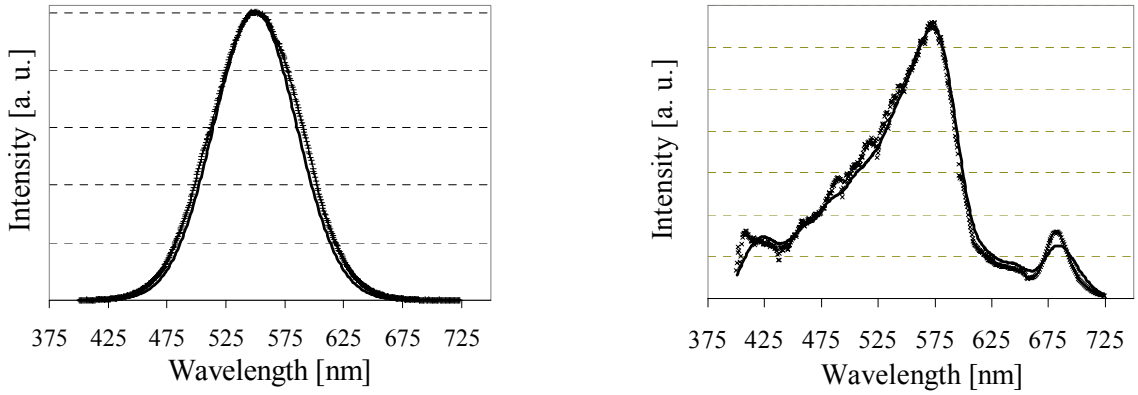

Fig. 7. Spectral matches of a visible STS to (left) Gaussian and (right) ocean color target spectral distributions. The dashed line is the target distribution; the solid line is the realized STS spectral distribution.

3. HYPERSPECTRAL IMAGE PROJECTOR

The HIP system is designed around commercial Digital Light Processing (DLP) projection systems. In these systems, shown schematically in Fig. 8 [10], light is focused through a rotating red, green, and blue filter wheel. The light then

homogenously illuminates a DMD-mirror array. Light from the DMD mirror array is projected onto a screen or other suitable medium. By varying the time that the mirrors are turned on within the period of time the light is incident on one of the three primary colors making up the filter wheel, different colors are projected onto different regions of the screen, making a full color image. In typical projection systems, scenes are updated at a rate of 50 Hz to 60 Hz.

The HIP system functions in the same basic fashion, with one notable difference. The three-color filter wheel is replaced by the STS source. Now instead of 3 fixed spectral distributions, we have external control over the spectral distributions input into the scene projector. Both the number of distributions and their spectral content can be varied at will. The basic layout of the HIP system is shown in Fig. 9. The STS is highlighted, circled on the left hand side of the figure, while the DMD projection system is circled on the right hand side of the figure. Instead of synchronizing the scene projector to a rotating filter wheel, the two DMD mirror arrays are synchronized.

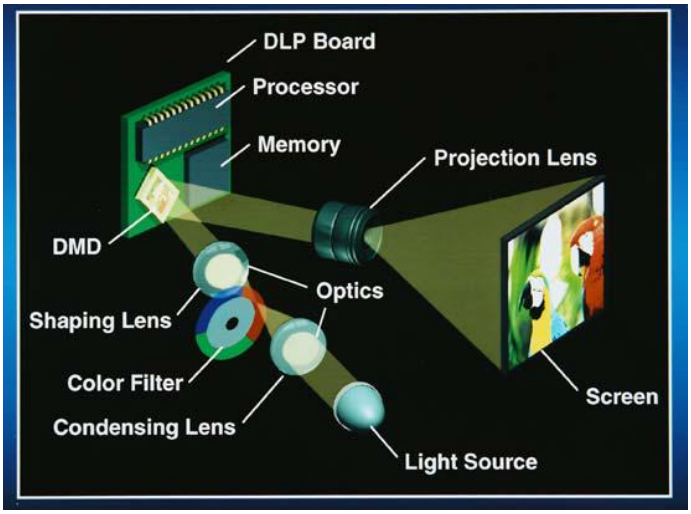

Fig. 8. Single chip DLP projection system layout [10]. The r,g, b basis functions are produced by a rotating color filter wheel.

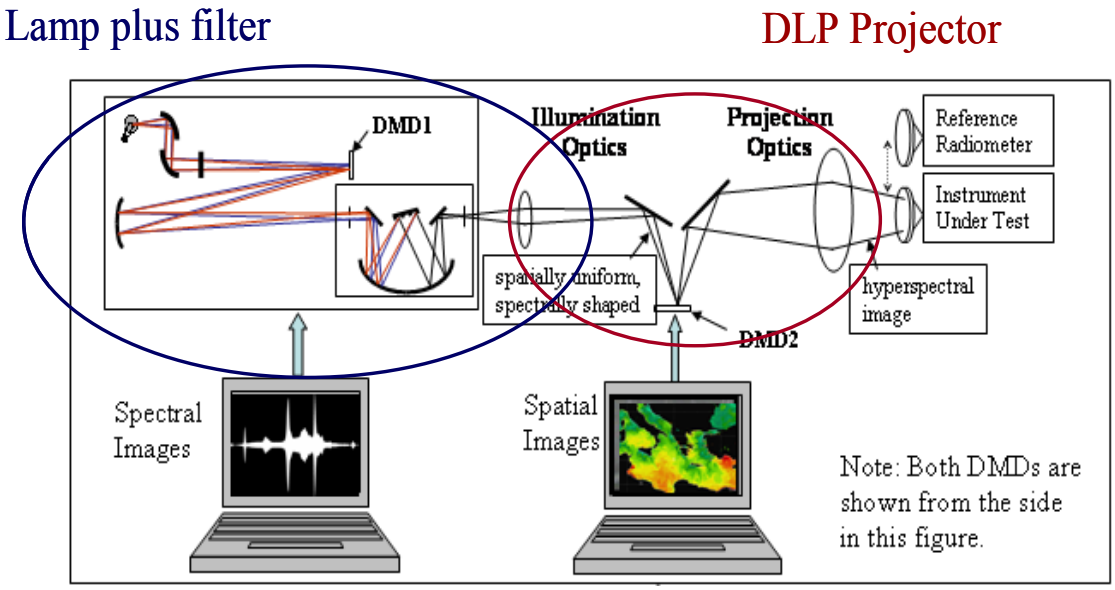

Fig. 9. HIP layout. The circled components are related to components of a standard DLP projection system. In this example, scenes are projected directly into the instrument under test.

In a standard DLP projection system, the 3 spectral distributions from the rotating filter wheel form the system's basis functions. The colors projected from the system are linear combinations of the 3 basis functions. Idealized basis functions from a standard DLP system used to create color scenes are shown in Fig. 10. In contrast to the conventional DLP system, 40, 10-nm-wide basis functions, for example, can be used in the HIP to create desired spectral distributions. Nineteen of those basis functions are shown in Fig. 11. The other basis functions are not shown for clarity. They lie between the shown basis functions. Note the difference in spectral coverage achievable using the two sets of basis functions. Instead of generating colored scenes, the HIP can create a scene with true spectral content using these basis functions, within the 10 nm resolution afforded by the basis functions chosen. Of course, if there is additional information about a particular scene, that information can be used to create more complex basis functions. Such a situation is shown in Fig. 12, where a hyperspectral image is deconvolved into its individual spectral components [11]. In this case, the image can be recreated using the six basis functions shown in the right hand side of the figure. In both examples, the goal is to create complex scenes in the laboratory with high fidelity spectral content.

Currently, we have created scenes with 3 STS basis functions using a prototype HIP projector. For additional details on the HIP, see reference [12].

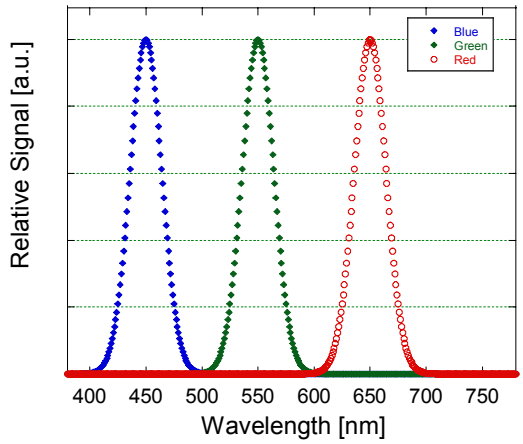

Fig. 10. DLP red, green, and blue basis functions.

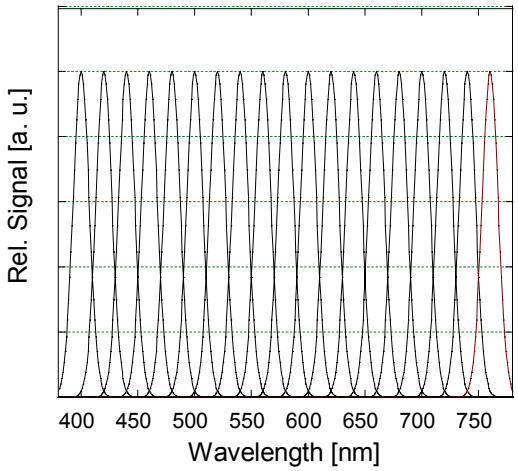

Fig. 11. Example basis functions from a HIP.

4. CONCLUSIONS

As remote sensing has advanced from imaging to hyperspectral imaging, two-dimensional images have been replaced by 3-dimensional hypercubes of data. The additional wealth of information in the data cubes provided by hyperspectral imagers has led to an increase in applications of remote sensing data in areas such as agriculture, mining, and environmental monitoring as well as climate change research. By analogy, in radiometry, with the development of HIP systems, we are transitioning from 'zero-dimensional' space to 'three-dimensional' space in terms of the spectral and spatial content in sources available for characterization and calibration. A fourth dimension (time) is also available with these platforms. The added sensor characterization and calibration flexibility provided by these platforms and the wealth of information generated using them should enhance pre-flight instrument characterization, validate calculated sensor performance, and ultimately improve on-orbit instrument performance as well as the quality of the data products produced by those sensors.

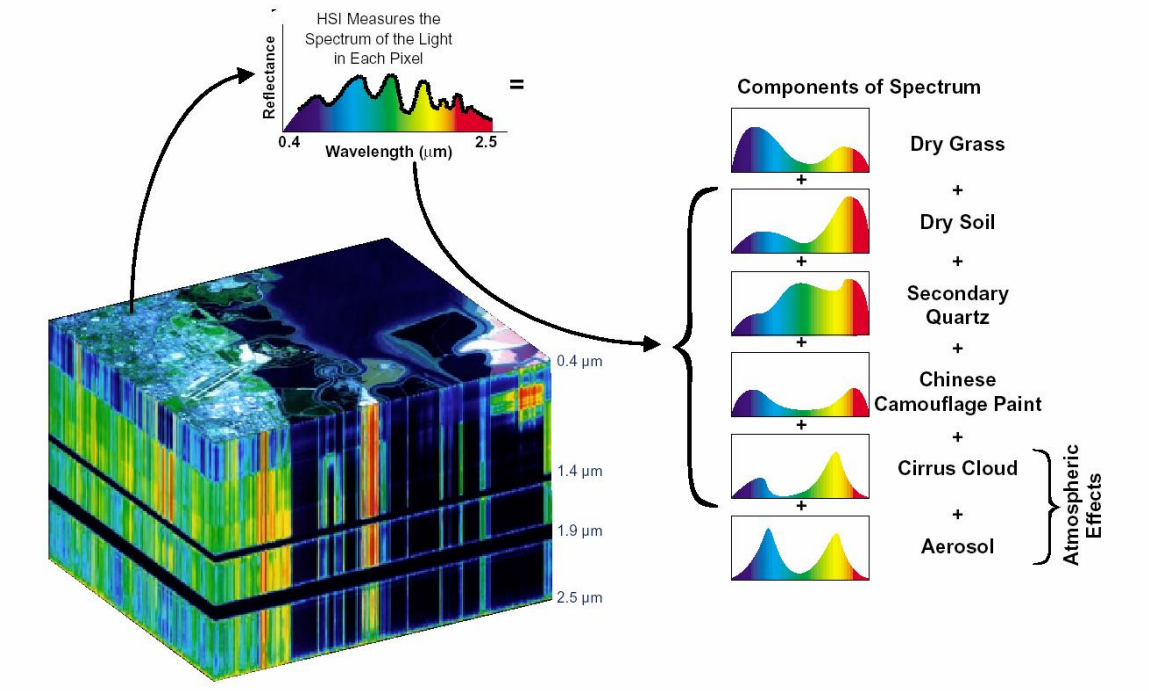

Fig. 12. Example set of scene basis functions based on hyperspectral measurement results [from Ref. 11]. The bottom left figure is a hypercube of data with spatial location given by the x and y axes and spectral information contained along the z-axis. The spectral distribution of one pixel is shown in the upper left hand corner and the components that make up that spectrum (along with their physical origin) are shown on the right hand side.

ACKNOWLEDGEMENTS

We would like to acknowledge the guidance and support for this work by Gerald T. Fraser. This work is funded in part by the NIST Office of Law Enforcement Standards (OLES).

Note: References are made to certain commercially available products in this paper to adequately specify the experimental procedures involved. Such identification does not imply recommendation or endorsement by the National Institute of Standards and Technology, nor does it imply that these products are the best for the purpose specified. DLP and DMD are trademarks of Texas Instruments, Inc.

REFERENCES

1. Guenther, B., et al., "MODIS Calibration: A brief review of the strategy for the at-launch calibration approach," *J. Atmos. Oceanic Tech.* **13**, 274-285 (1996).
2. Barnes, R. A., A. W. Holmes, W. L. Barnes, W. E. Esaias, C. R. McClain, and T. Svitek, 1994: SeaWiFS Prelaunch Radiometric Calibration and Spectral Characterization, NASA Tech. Memo. 104566, Vol. 23, S.B. Hooker, E.R. Firestone, and J.G. Acker, Eds., NASA Goddard Space Flight Center, Greenbelt, Maryland, 55 pp.
3. Mango, S. A., R. E. Murphy, H. Ouaidrara, and W. P. Menzel, "NPOESS Preparatory Project (NPP) instrument characterization and calibration, and products validations: An integrated strategy in preparation for NPOESS new generation of environmental satellites," *Proc. SPIE* **4891**, 22-35 (2003).

4. Ohring, G., B. Wielicki, R. Spencer, B. Emery, and R. Datla, eds., Satellite instrument calibration for measuring global climate change, NISTIR 7047, U.S. Department of Commerce, Technology Administration, Washington, DC, 2004, 102 pp.
5. Rice, J. P., S. W. Brown, B. C. Johnson, and J. E. Neira, "Hyperspectral image projectors for radiometric applications," *Metrologia* **43**, S61-S65 (2006).
6. MacKinnon, N., U. Stange, P. Lane, C. MacAulay, and M. Quatrevalet, "Spectrally programmable light engine for in vitro or in vivo molecular imaging and spectroscopy," *Appl. Opt*. **44**, 2033-2040 (2005).
7. Fryc, I., S. W. Brown, G. P. Eppeldauer, and Y. Ohno, "A spectrally tunable solid-state source for radiometric, photometric and colorimetric applications," *Proc. SPIE* **5530**, 150-156 (2004).
8. Brown, S. W., J. P. Rice, J. D. Jackson, J. E. Neira, B. C. Johnson, "Spectrally tunable sources for advanced radiometric applications," *J. Res. Natl. Inst. Stands. Technol.* (2006), in press.
9. http://www.fianium.com/products/sc.htm
10. http://www.dlp.com
11. http://www.silvereng.com/PDF/NEMO.pdf
12. Rice, J. P., S. W. Brown, and J. E. Neira, "Development of hyperspectral image projectors," *Proc. SPIE* (2006), in press.